The Astrophysical Journal, 759:22 (7pp), 2012 November 1 doi:10.1088/0004-637X/759/1/22

SEEKING COUNTERPARTS TO ADVANCED LIGO/Virgo TRANSIENTS WITH *SWIFT*

Jonah Kanner[1], Jordan Camp[1], Judith Racusin[2], Neil Gehrels[2], and Darren White[3]
[1] NASA Goddard Space Flight Center, Mail Code 663, Greenbelt, MD 20771, USA; jonah.b.kanner@nasa.gov
[2] NASA Goddard Space Flight Center, Mail Code 661, Greenbelt, MD 20771, USA
[3] Department of Physics and Astronomy, University of Sheffield, Hicks Building, Hounsfield Road, Sheffield S3 7RH, UK
Received 2012 August 7; accepted 2012 September 7; published 2012 October 12

ABSTRACT

Binary neutron star (NS) mergers are among the most promising astrophysical sources of gravitational wave (GW) emission for Advanced LIGO and Advanced Virgo, expected to be operational in 2015. Finding electromagnetic counterparts to these signals will be essential to placing them in an astronomical context. The *Swift* satellite carries a sensitive X-Ray Telescope (XRT), and can respond to target-of-opportunity requests within one to two hours, and so is uniquely poised to find the X-ray counterparts to LIGO/Virgo triggers. Assuming that NS mergers are the progenitors of short gamma-ray bursts (GRBs), some percentage of LIGO/Virgo triggers will be accompanied by X-ray band afterglows that are brighter than 10^{-12} erg s^{-1} cm^{-2} in the XRT band one day after the trigger time. We find that a soft X-ray transient of this flux is bright enough to be extremely rare, and so could be confidently associated with even a moderately localized GW signal. We examine two possible search strategies with the *Swift* XRT to find bright transients in LIGO/Virgo error boxes. In the first strategy, XRT could search a volume of space with a ∼100 Mpc radius by observing ∼30 galaxies over the course of a day, with sufficient depth to observe the expected X-ray afterglow. For an extended LIGO/Virgo horizon distance, the XRT could employ 100 s exposures to cover an area of ∼35 deg^2 in about a day and remain sensitive enough to image GW-discovered GRB afterglows. These strategies demonstrate that discovery of X-ray band counterparts to GW triggers will be possible, though challenging, with current facilities.

Key words: galaxies: statistics – gamma-ray burst: general – gravitational waves – X-rays: general

Online-only material: color figures

1. INTRODUCTION

The construction of the Advanced LIGO and Advanced Virgo[4] gravitational wave (GW) observatories is in progress, with completion expected as early as 2015 (Harry & LIGO Scientific Collaboration 2010; Accadia et al. 2012). These detectors are expected to serve as all-sky monitors for mergers of binary neutron stars (NS–NS), mergers of neutron stars with stellar-mass black holes (NS–BH), and mergers of binary black holes. The detectors are designed to observe NS–NS mergers to an average distance of 200 Mpc, and NS–BH mergers to 400 Mpc (Abadie et al. 2010). The GW signal from such events could provide a wealth of information, including the masses and spins of the component objects, and an estimate of the luminosity distance to the source. However, this network of GW detectors will have, even in the best case scenarios, only modest localization ability. This means that placing a GW observation in an astronomical context, including identification of a host galaxy and environment, will require finding a counterpart electromagnetic (EM) signal to the merger event. A joint EM/GW observation would describe an explosive event in unprecedented detail, since the GW signal would directly probe the progenitor's dynamics while the EM signal would carry information on the environment and allow improved parameter estimation. Moreover, a population of such joint EM/GW signals could be used to estimate cosmological parameters (Dalal et al. 2006; Nissanke et al. 2010).

The main challenge in the identification of an EM counterpart to an observed GW signal will be the large positional uncertainty associated with current networks of GW observatories. The positional uncertainty for a given event will depend strongly on a number of factors, including signal-to-noise ratio (S/N), position on the sky, available position reconstruction algorithms, and the internal state of the GW network. As designed, all three detectors in the Advanced LIGO/Virgo network would operate at a similar sensitivity, leading to typical positional uncertainties around ∼20 deg^2 (Klimenko et al. 2011; Fairhurst 2011; Nissanke et al. 2011). On the other hand, studies using data from the last science runs of LIGO and Virgo have shown uncertainties for low S/N signals of 50–200 deg^2 (Abadie et al. 2012b), during times when detectors differed by a factor of ∼2 in amplitude sensitivity. During the early years of observing with the second generation network, evolving sensitivity levels will likely lead to variation in the ability to localize sources.

Since there have been no certain observations of stellar-mass compact object mergers, predicting the wavelength, flux, and duration of a possible EM signal is somewhat speculative. However, some models seem promising. NS–NS mergers and NS–BH mergers are both possible progenitors for short gamma-ray bursts (GRBs; Fox et al. 2005; Gehrels et al. 2005), and both their prompt emission and afterglow have been carefully studied. In addition, theoretical considerations and simulations lead to the expectation of an isotropic, optical signal that results from energy released in decays of unstable isotopes following *r*-process nucleosynthesis (Metzger et al. 2010; Roberts et al. 2011; Piran et al. 2012). Some consideration has already been given to observing strategies that might discover an optical or radio band counterpart to a merger event (Metzger & Berger 2012; Coward et al. 2011), and searches have been performed in a range of wavelengths on low-threshold triggers from the initial LIGO/Virgo network (Evans et al. 2012; Abadie et al. 2012b, 2012a). Past searches have also sought coincident triggers using archived GRB and GW data (Abadie et al. 2012c). In this work, we focus on the X-ray band, and consider the *Swift* satellite

[4] https://tds.ego-gw.it/itf/tds/file.php?callFile=VIR-0027A-09.pdf

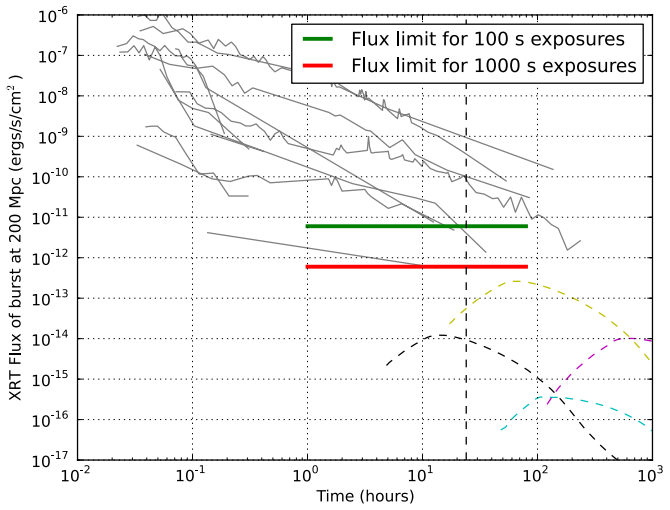

Figure 1. Gray curves are XRT light curves for short GRBs with known redshifts, scaled to a distance of 200 Mpc (Evans et al. 2007, 2009). The green line shows the XRT flux limit for 100 s exposures, which could cover ∼35 deg^2 in one day, and the green line indicates the limit for a 1000 s exposure. Some observed afterglows quickly fade, and so are not observable 1 hr after the burst. However, the "long-lived" afterglows are generally bright enough to be observed 10–100 hr after the burst, even with short (∼100 s) exposures. The dashed, colored curves show predicted light curves for off-axis light curves viewed at twice the jet opening angle, scaled to 200 Mpc (van Eerten & MacFadyen 2011). The simulated light curves have jet energies of 10^{48} and 10^{50} erg, and circumburst medium number densities of 1 cm^{-3} and 10^{-3} cm^{-3}.

(A color version of this figure is available in the online journal.)

(Gehrels et al. 2004) as a potential instrument for discovering EM signals following a trigger from the second generation LIGO/Virgo network.

Swift has an unmatched record as an engine for producing observations of GRBs and their afterglows. In the typical mode of discovery, *Swift*'s Burst Alert Telescope (Barthelmy et al. 2005) sweeps the sky for GRBs. When a GRB is discovered, the X-Ray Telescope (XRT; Burrows et al. 2005) and UV/Optical Telescope (UVOT; Roming et al. 2005) are automatically slewed to the estimated source position. This strategy has been extremely successful: the XRT finds soft-band X-ray counterparts to nearly 80% of observed short GRBs with prompt observations. For comparison, optical band counterparts are only discovered for ∼30% of short GRBs. If we accept the putative link between compact object mergers and short GRBs, then the XRT band (0.3–10 keV) seems a natural place to find the counterparts to compact object mergers.

2. SOURCES

2.1. GRB Afterglows

The collection of short GRB afterglows observed with *Swift* and with measured redshifts has been studied by Racusin et al. (2011). The late-time X-ray afterglows decay with a power law $t^{-\alpha}$, with a temporal index $\alpha \sim 1.5$ and at 1 day after the trigger time, show luminosities in the XRT band ranging from 10^{42} to 10^{45} erg s^{-1}. Placing these afterglows at a luminosity distance of 200 Mpc leads to fluxes of between 10^{-12} and 10^{-9} erg s^{-1} cm^{-2} (see Figure 1). The XRT routinely observes these objects out to a redshift of $z \sim 0.5$, suggesting that the afterglows from sources within the GW detector horizon (∼400) Mpc would be relatively bright.

An important feature of afterglows in this context is that they are expected to be beamed. This has the implication that only a small fraction, f_b, of NS–NS or NS–BH mergers will have a beam pointed toward Earth. For small jet opening angles, f_b is related to the jet opening half-angle as $f_b \sim \theta_j^2/2$. The jet angle is highly uncertain, but is typically expected to be between a few degrees and a few tens of degrees, meaning that f_b is likely of the order of 1%. If this is the case, then there is a major implication for LIGO/Virgo triggers: the vast majority of them will not be associated with on-axis GRBs. However, the fraction of GW-selected events within the beam will likely be larger than f_b due to a particular bias (Schutz 2011; Nissanke et al. 2010). Inspiraling compact objects emit GW energy preferentially in the direction parallel to their angular momentum axis, that is, the GWs are weakly beamed in the same direction as the GRB jet. Schutz (2011) shows that this effect will increase the fraction of GW-selected compact object mergers with their beam pointed toward earth by a factor of 3.4 over the strictly geometric prediction. Moreover, a few short bursts have lower limits on their jet opening angles placed above 10 deg (Racusin et al. 2011; Fong et al. 2012; Coward et al. 2012). If we estimate the opening angle of short GRBs as around 10 deg, then the expected fraction of LIGO/Virgo observed mergers with earth within the jet is ∼5%, or one observable GRB in every ∼20 LIGO/Virgo observed NS–NS mergers.

The above estimate of f_b is highly uncertain, due to the limited number of observations of short GRB jet breaks. On the other hand, it is possible to make a reasonably robust estimate of the number of short GRBs within the LIGO/Virgo range, based on the observed rates of GRBs (Chen & Holz 2012; Metzger & Berger 2012; Abbott et al. 2010). The main source of uncertainty is then the progenitor of short bursts. If we assume that all short GRBs are due to NS/NS mergers, then we expect 0.3–3 events to be in range per year with Advanced LIGO design sensitivity. However, the LIGO range for BH/NS events is greater by a factor of ∼2, leading to 2–20 events per year if we assume that all short GRBs are caused by NS/BH mergers. In the early years of Advanced LIGO, with half the design range, we might then expect ∼0.1 GW/GRB coincidences per year under the NS/NS assumption, or ∼1 such event per year under the BH/NS assumption. Uncertainties include the possible gain in reach of the GW instruments due to reduced background with a coincident GRB observation, or factors accounting for the less-than-perfect spatial and temporal coverage of both GRB and GW monitors.

Even if a short GRB is beamed in a direction away from the earth, X-ray band emission from the afterglow may be visible in the direction of earth. There are no confirmed observations of such off-axis afterglows, presumably due to the difficulty in reliably identifying them in all-sky survey data. However, some predicted light curves from off-axis afterglows are available from simulations by van Eerten & MacFadyen (2011). In order to compare the simulation results with observed, on-axis light curves, we scale the results to a luminosity distance of 200 Mpc, and calculate the XRT band flux assuming a power law spectrum with an index of 1.5 (see Figure 1). Comparing off-axis light curves with observations of GRBs (where the observer is inside the jet opening angle) suggests that the off-axis observer will encounter a number of challenges seeking an X-ray counterpart. For an observer located at twice the jet opening angle, there is a brightening time of between two and twenty days, so a wait of at least several days would be needed to observe an off-axis afterglow in X-rays. A large time window between the GW trigger and the observation of the counterpart would make establishing a connection difficult. Moreover, the off-axis

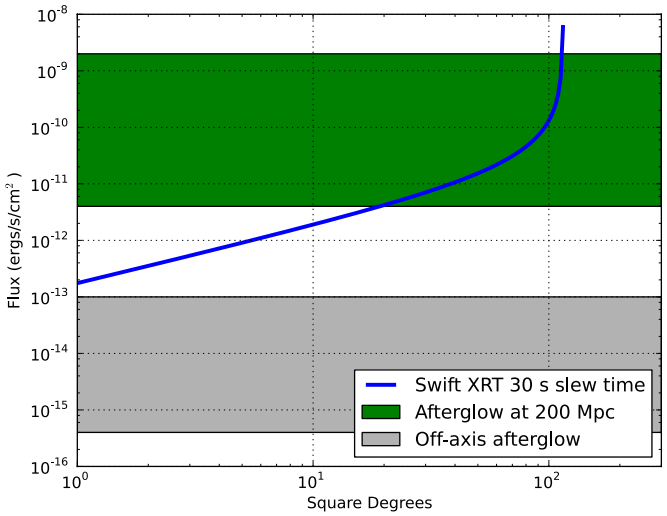

Figure 2. Plot showing the potential for a large area survey with XRT over the course of a single day. Enough exposures are taken over the course of 24 hr to cover the area shown on the horizontal axis, under the assumption that the XRT requires 30 s of slew and settle time for each image. For comparison, the range of fluxes of short GRB afterglows, scaled to one day after the trigger time and a luminosity distance of 200 Mpc, is shown as the green shaded region. The gray region shows the peak XRT flux of a range of off-axis light curves, also scaled to 200 Mpc. The peak flux of the model off-axis light curves occurs several days after the GRB trigger time.

(A color version of this figure is available in the online journal.)

emission is considerably dimmer than the on-axis emission, by several orders of magnitude (see Figure 2). In addition to being more difficult to detect, the fainter emission will also be more difficult to separate from background variability. This suggests that an observation of an off-axis afterglow would require an exceptionally nearby NS–NS merger. For a merger at 50 Mpc, the peak flux of an X-ray afterglow observed at twice the jet opening angle would range $\sim 10^{-15}$–10^{-13} erg s^{-1} cm^{-2}, and so could be observable in a 10 ks XRT exposure. Such events are likely to be rare, perhaps once every 10–20 years based on observed GRB rates. However, they present an interesting possibility, since the large S/N that they would produce in the Advanced LIGO/Virgo network would allow for exceptional localization and parameter estimation.

2.2. Kilonovae

While observing the afterglow to a short GRB from a position outside the beam will likely be challenging, another source of emission from NS–NS mergers may create an isotropic transient. Though lacking in observational evidence, transients known as kilonovae have been treated in the literature by several authors (Metzger et al. 2010; Roberts et al. 2011; Li & Paczyński 1998; Kulkarni 2005; Goriely et al. 2011). The model predicts that ejecta from the merger will grow heavy nuclei through *r*-process nucleosynthesis, which subsequently decay and heat the material. The thermal emission leads to an optical band transient with a peak luminosity around one day after the merger event, and a dimming over the course of the next few days. The transient may have a blue color, with *U*-band emission that appears brighter and peaks sooner than the *R*-band emission. Because this mechanism is largely independent of the environment around the merger, and leads to isotropic emission, it is possible to imagine that a large fraction of NS–NS and NS–BH mergers are accompanied by observable kilonovae. A kilonova at 200 Mpc is expected to peak around magnitude 19–22: bright enough to be detected by the UVOT instrument on *Swift*. UVOT is aligned in parallel to the XRT, so a search over one or two days for X-ray afterglows with *Swift* is a simultaneous search for optical band kilonovae. It should be noted that *Swift*'s capability in searching for optical band transients is not unique; ground-based optical survey telescopes can also search large areas to these magnitudes (Metzger & Berger 2012).

3. SEARCH STRATEGIES WITH *SWIFT*

The large position uncertainty associated with LIGO/Virgo triggers matches well onto the capabilities of ground based, large area survey projects such as PTF, Pan-STARRS, QUEST, and SkyMapper (Metzger & Berger 2012). However, a space-based X-ray facility may present some unique advantages. The X-ray afterglows to short GRBs are easily distinguished from other X-ray sources both by their large flux and characteristic power-law dimming. A space-based, as compared to a ground-based, facility also has the advantage that wait time for a source to pass overhead is typically ∼90 minutes instead of ∼12 hr, and the sky coverage is nearly total, where a ground based facility has access to a smaller fraction of the sky.

The combination of fast response times to target-of-opportunity (TOO) requests (around one or two hours), and a long heritage with GRB afterglows makes the *Swift* satellite a natural facility to consider. Much of the following discussion could apply to other facilities as well, particularly *XMM-Newton* and *Chandra*, however, the fast TOO response may make *Swift* the only practical choice for seeking quickly fading counterparts. With this in mind, and with the intention of making the discussion as concrete as possible, we focus specifically on the *Swift* observatory.

3.1. Searching the Full Error Box

The first strategy that we consider is using the *Swift* XRT to tile an entire LIGO/Virgo error box. Estimates for the uncertainty associated with a LIGO/Virgo position reconstruction vary from a few tens of square degrees to over a hundred square degrees (Abadie et al. 2012b; Nissanke et al. 2011; Klimenko et al. 2011; Fairhurst 2011). In fact, the precision of any particular position estimate will depend on a number of factors, including S/N and sky position. Certainly, any position reconstruction with the LIGO/Virgo network will cover an area significantly larger than the 0.16 deg^2 XRT field of view (FOV). In order to evaluate the feasibility of search strategies, we consider 100 deg^2 as a nominal value for the LIGO/Virgo position uncertainty.

To characterize the ability of the XRT to quickly survey a large area, we write the limiting flux of an observation as a function of observing time as

$$F = 6 \times 10^{-12} \left(\frac{100\,\mathrm{s}}{T} \right) \mathrm{erg\ s^{-1}\ cm^{-2}}, \quad (1)$$

where T is the observing time (Moretti et al. 2007). This is valid in the regime of photon limited exposures ($T < 10^4$ s), and assumes that 12 counts are needed for a detection, with a conversion factor between count rate and flux of 5×10^{-11}. If we imagine that the sought afterglow to a GW trigger is visible for roughly one day, then we can calculate how much observing time, and hence what limiting flux, we can associate with observations covering various amounts of area:

$$T = \left(\frac{86{,}400\ \mathrm{s}}{3} \right) \left(\frac{0.12\ \mathrm{deg}^2}{\mathrm{Area}} \right) - S \quad (2)$$

$$F \approx 2 \times 10^{-14} \left(\frac{\text{Area}}{0.12 \text{ deg}^2} \right) \text{erg s}^{-1} \text{ cm}^{-2}, \quad (3)$$

where S represents the amount of time for each slew and settle of the instrument. Equation (3) assumes that the observing time is much larger than the total slew time. The factor of 1/3 is to account for the fact that most observations cannot continue over an entire orbit, due primarily to occultation by the earth. In addition, the size of the FOV has been reduced to 0.12 deg^2 to allow some overlap in the tiling pattern. The resulting limiting fluxes are plotted in Figure 2 for a range of areas, with S set to 30 s.

Under these assumptions, the XRT might take a series of 290 exposures, each 100 s long. This would cover 35 deg^2 in about one day, and yield a flux limit of around 6×10^{-12} erg s^{-1} cm^{-2}. With the current on-board software, this could be accomplished with 8 applications of the programmed 37 tile pattern. The resulting flux limit seems to be sensitive enough to find most on-axis afterglows, but not predicted off-axis afterglows for most viewing angles.

Clearly, this approach would be less strenuous if the position uncertainty associated with a particular event could be reduced. Some estimates predict that 100 deg^2 is a conservative estimate, and suggest 20–40 deg^2 as more typical numbers, depending on underlying signal models and algorithm. For example, Nissanke et al. (2011) predict that, using a Markov Chain Monte Carlo parameter estimation technique, only 36 deg^2 of area need to be searched to recover 70% of binary mergers detected with an S/N of at least 6 at all 3 detector locations, or 12 deg^2 could be searched for a 50% recovery rate. The addition of a fourth GW detector to the network could also improve localization ability to around 10 deg^2. KAGRA (Kuroda & LCGT Collaboration 2010) located in the Kamioka mine in Japan could be operational by 2018, and a third LIGO site in India[5] could be operational by 2022.

An important consideration in searching a large area for a single event is to understand if we can distinguish the event from other sources. For the case where the error box is out of the galactic plane, some suggestive numbers are shown in Figure 3. At a sensitivity of 2×10^{-12} erg s^{-1} cm^{-2}, a typical area of 100 deg^2 would find only a few extragalactic sources (Puccetti et al. 2011; Mateos et al. 2008). Demanding variability in the source should be a strong handle for cutting this number down further. The black dashed curve uses statistics of observed active galactic nucleus (AGN) variability to forecast how many variable AGNs are likely to fluctuate by a factor of two or more between two images (based on numbers found in Gibson & Brandt 2012). The study represented as a blue triangle found a similar number density by systematically searching the RASS data for variable sources with a "flare"-like light curve (Fuhrmeister & Schmitt 2003). The red star shows the result of another RASS study that used stronger cuts to seek GRB orphan afterglows (Greiner et al. 2000). The three orders of magnitude in density reduction between this point and the number of AGNs was achieved by demanding that no X-ray source was present at the location of the transient either before or after the flare event. This seemed to be a very powerful cut, and resulted in finding around 1 source in every 10,000 deg^2, or a 1% chance of finding an unrelated afterglow like source in association with the 100 deg^2 GW error box. When seeking only afterglows within a limited distance range, it is possible

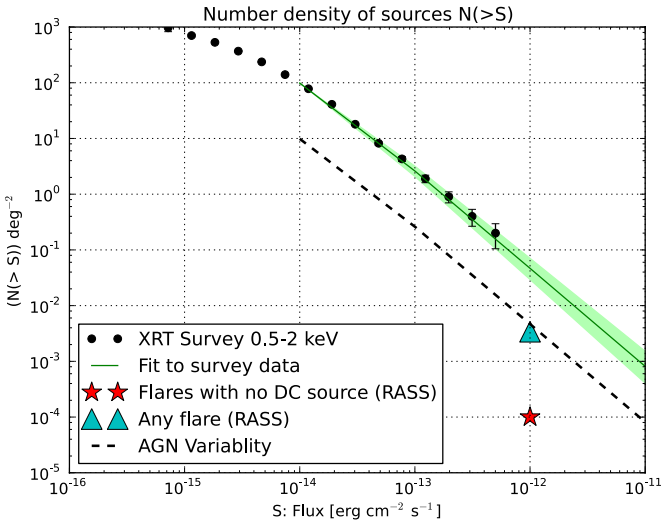

Figure 3. Extragalactic X-ray background number density estimated in various ways. The black points show the observed number density at high galactic latitude in the *Swift* serendipitous survey, with a fit shown in green (Puccetti et al. 2011). The black dashed line is an estimate of the number of variable AGNs that may be mistaken as transients, assuming a reference image that is twice the depth of the limit shown on the x-axis Gibson & Brandt (2012). The triangle marks the density of variable "flare like" sources in the ROSAT All-Sky Survey (Fuhrmeister & Schmitt 2003), and the red star marks the density of candidate orphan afterglows found in a *ROSAT* data (Greiner et al. 2000).

(A color version of this figure is available in the online journal.)

to remove the majority of flare stars by demanding a spatial coincidence between the transient source and an optical galaxy. This suggests that a transient, soft X-ray source, brighter than $\sim 10^{-12}$ erg s^{-1} cm^{-2} found in connection to a GW trigger is likely to be associated. The expectation that some LIGO/Virgo triggers will have short-lived, soft X-ray counterparts brighter than anything else within the error box suggests that a wide-field, focusing instrument in this band would be a useful follow-up tool.

A LIGO/Virgo trigger in temporal coincidence with a *Fermi* GBM (Meegan et al. 2009) trigger would be of great interest. GBM sees a large fraction of the sky (~65%; Meegan et al. 2009), and so this is a likely scenario. The GBM has a large uncertainty in its position reconstruction (Briggs et al. 2009). For example, in the GBM burst catalog (Paciesas et al. 2012), the listed short bursts have a median positional uncertainty of 7.5 deg. Some of this error (~3 deg) is due to systematics in the localization process (Hurley et al. 2011; Paciesas et al. 2012).

A GW trigger in coincidence with a *Fermi* GRB observation would definitively establish the progenitor of the burst. However, the large error radius associated with *Fermi* means that a GBM trigger alone could not provide a host galaxy identification or provide the coordinates of the potential afterglow. Given the high degree of interest in such an event, seeking the afterglow and host galaxy seems well worth the effort. The range of typical GBM position uncertainties (3–12 deg; see Figure 4) overlaps the range of positional errors with LIGO/Virgo, with a median position uncertainty of 7.5 deg, or 176 deg^2 under the assumption of a circular region. While these uncertainties may often be larger than the GW position uncertainties, in the early days of advanced detectors, it is possible that the three GW detectors will have unequal sensitivities. This would lead to GW error boxes that are very spread out on the sky. For example, if only two detectors are operating at the time of an event, then the GW network will localize the event to a ring on the sky of the

[5] https://dcc.ligo.org/cgi-bin/DocDB/ShowDocument?docid=91470

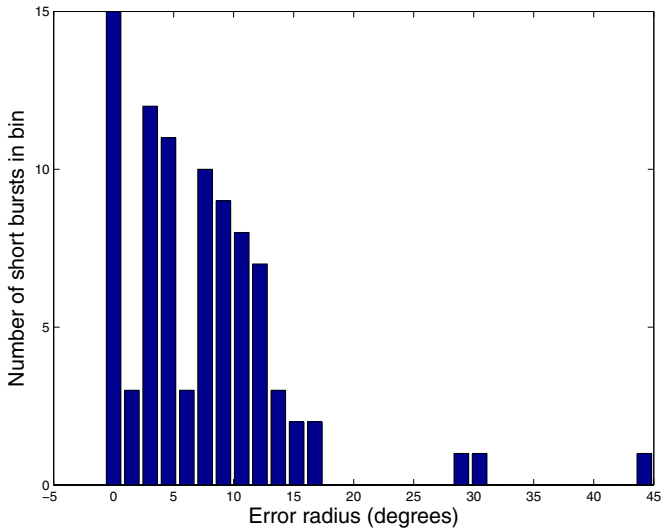

Figure 4. Distribution of estimated error radii for 88 bursts from the *Fermi* GBM Burst Catalog. The bursts are selected only with the criteria that $T_{90} < 2$ s. The *x*-axis is in degrees, the *y*-axis is the number of bursts in the bin. Many of the bursts in the 0 bin have position information that is known from some other source, such as the *Fermi* Large Area Telescope or *Swift*.

(A color version of this figure is available in the online journal.)

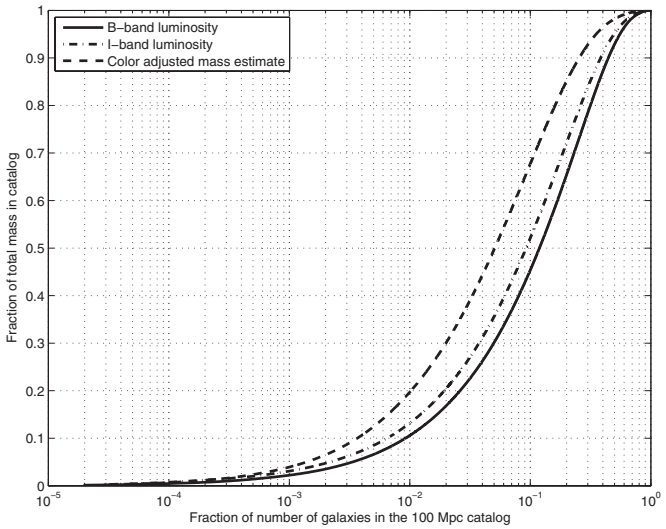

Figure 5. GWGC contains roughly 53,000 galaxies within 100 Mpc of earth. The plot shows what fraction of the total number of galaxies must be selected in order to obtain a target fraction of the total luminosity or mass in the catalog. Only 10% of the galaxies contain 50% of the *I*-band luminosity. Including 90% of the blue light luminosity requires 40% of the number of galaxies. The distribution of the color adjusted mass estimate suggests that even a smaller fraction of galaxies in the catalog may contain a given fraction of the total mass, however, this may be an effect of color scatter due to metallicity.

order of 1000 deg^2. In such a scenario, the *Fermi* error ellipse would be more constraining for the LIGO/Virgo uncertainty region. It is also possible to imagine taking the intersection of the GBM error ellipse and the LIGO/Virgo skymap.

3.2. Searching with a Galaxy Catalog

The fact that the LIGO/Virgo network is sensitive to only a limited distance can be used to dramatically reduce the amount of area that must be searched for an EM counterpart. Merger events should occur within, or close to, their host galaxies. In fact, Berger (2011) has found that short GRBs seem to track the total mass of galaxies. So, in response to a LIGO/Virgo trigger, it may be possible to search only the locations of known galaxies within a fixed distance horizon rather than the entire error box. This method was applied in efforts to search for EM afterglows to GW triggers using the initial LIGO/Virgo network (Kanner et al. 2008; Abadie et al. 2012b). For the 2009–2010 search, a galaxy catalog was constructed from publicly available information, known as the GW Galaxy Catalog (GWGC; White et al. 2011). This approach takes advantage of the limited distance reach of the GW instruments to merger events, in the sense that the sky is relatively sparse in galaxies to a limited distance range. In the limit of a GW detector that could observe events anywhere in the observable universe, this would clearly not be the case, and the density of observable galaxies on the sky would make a galaxy catalog ineffective in limiting the amount of sky area to be observed. The question that we ask is: out to what distance reach is a galaxy catalog still useful in this way with the *Swift* XRT?

A similar question was addressed by Nuttall & Sutton (2010), who found that the galaxy catalog can be an extremely useful tool in recovering the true location of a GW inspiral signal out to at least 100 Mpc, even if only a few galaxies are imaged. Here, we attempt to find the limiting range where searches with and without a galaxy catalog require the XRT to observe the same amount of sky area.

Past counterpart searches using a galaxy catalog assumed that the likelihood of a merger event in the galaxy traces either the mass or the star formation rate of the galaxy (Abadie et al. 2012a, 2012b). Competing models exist for which types of galaxies are more likely to host merger events (O'Shaughnessy et al. 2010). In order to explore the implications of various models, we have used the HyperLeda database to add measurements of *I*-band (near-infrared) luminosity to the GWGC. This resulted in a catalog with 51,136 objects with *B*-band measurements, 34,363 objects with *I*-band measurements, and 31,732 galaxies with both *I*-band and *B*-band measurements. The *B*-band luminosity is estimated to be ∼60% complete (White et al. 2011). Conventional wisdom suggests that wavelengths in the near-infrared should be good tracers of total stellar mass. However, the application of a color correction has been shown to improve mass estimates in some cases (Bell & de Jong 2001; Bell et al. 2003).

Adopting the model presented in Bell & de Jong (2001), we constructed a color corrected mass estimate using the *I*-band magnitude and $[B - I]$ color for each galaxy in our sample with both measurements. We applied the model as

$$\log_{10}(M/L) = -0.88 + 0.60[B - I], \quad (4)$$

where M and L are the galactic mass and *I*-band luminosity, both in solar units. Bell et al. (2003) showed that in near-infrared wavelengths, this color dependency is likely too steep, but did not provide corrected values for *I*-band measurements. For this reason, it is likely that our color corrected mass estimate amplifies the effects of color scatter due to metallicity variations between galaxies, and so results in an artificial broadening in the distribution of masses in the catalog. The effect was partially mitigated by removing galaxies with colors far from the center of the distribution.

In the GWGC, out to 100 Mpc, there is roughly 1.3 possible host galaxies per square degree, or 130 possible hosts for a typical LIGO/Virgo error box. However, if we take the position that only enough possible hosts need to be imaged to make including the true host likely, then we can reduce this number further. Figure 5 shows that, averaged over the sky, 40% of

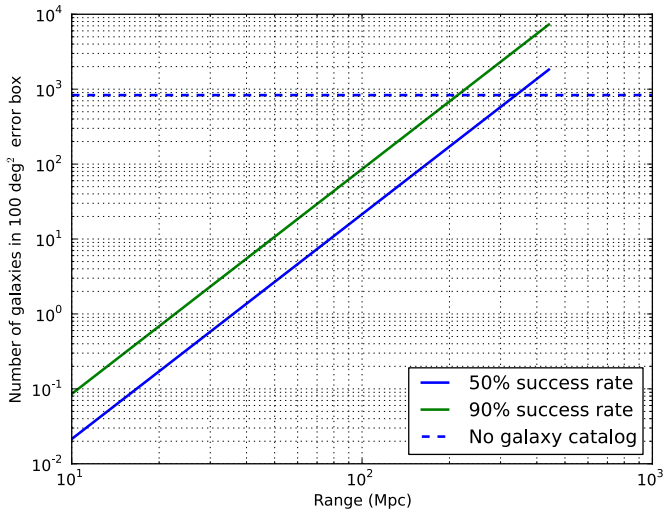

Figure 6. GWGC contains 53,000 galaxies within 100 Mpc of earth. The figure assumes that the number of galaxies within a horizon distance r scales as r^3, and that the catalog is 60% complete. Within a 100 Mpc horizon distance, imaging the galaxies needed to contain 90% of the I-band luminosity within a 100 deg^2 LIGO/Virgo error box requires an order of magnitude less pointings of the XRT than the number required to tile the whole LIGO/Virgo error box. The limit where a galaxy catalog is no longer useful seems to be around 200 Mpc. For comparison, the design curve for Advanced LIGO predicts a sky average NS–NS average range of around 200 Mpc. Initial LIGO had a sky average range of around 20 Mpc for NS–NS mergers.

(A color version of this figure is available in the online journal.)

galaxies contain 90% of the I-band luminosity. After adjusting for the completeness fraction of the catalog, this means a 100 deg^2 LIGO/Virgo error box with a 100 Mpc range could be covered at the 90% level by observing ∼90 galaxies, or at the 50% level by observing ∼20 galaxies. This represents dramatically fewer pointings of the *Swift* XRT than the 800 fields required to tile the whole error box. So, for a search with a range of 100 Mpc, the galaxy catalog still seems to be a useful tool. This suggests that in the early months of Advanced LIGO/Virgo, when horizon distances are expected to be below the design goals, a reasonable strategy would utilize exposures of roughly 1 ks, allowing the XRT to image 2 galaxies per orbit, and so observe 32 galaxies in a 24 hr period. Repeating the observations over a second, not necessarily concurrent, day would allow image subtraction with the UVOT to enable a search for kilonovae. However, it is important to note that this scenario is limited to the assumption of an NS–NS merger: BH–NS mergers have horizon distances that are greater by roughly a factor of two. Moreover, it is important to distinguish between the sky-averaged range distance, which we have used here, and the optimal horizon distance, which differ by a factor of 2.26.

In the case of a very nearby source (<100 Mpc), it may be possible to limit observations to only a few galaxies. In such cases, the search might be optimized for off-axis afterglows by taking longer, ∼10 ks exposures of each galaxy, over a span of a few days. This would result in flux limits of around 2×10^{-14} erg s^{-1} cm^{-2}, and so be deep enough for the more optimistic off-axis afterglow models.

No galaxy catalog is currently complete to 200 Mpc, although there are efforts underway to obtain one by the time of Advanced LIGO (M. Kasliwal 2012, private communication). Using the GWGC, a geometric scaling allows us to anticipate the result for a 200 Mpc horizon distance (see Figure 6). At 200 Mpc, if we still hope to capture the true source with a 90% likelihood, and assuming a similar distribution of galactic luminosities as those already contained in the GWGC, then the requirement is to observe around 700 galaxies per LIGO/Virgo trigger. This number is similar in scale to the 800 fields required to tile the whole error box, so we conclude that the limit of usefulness of a galaxy catalog for 24 arcmin fields is around 200 Mpc (see Figure 6).

Another important concern related to the application of a galaxy catalog is the possibility that NS–NS or NS–BH mergers will occur *outside* of their host galaxies. Asymmetries in the supernova that forms a compact object can impart a net momentum, or "natal kick," to the resulting NS or BH. If the kick is large enough to unbind the system from the gravitational potential of its host galaxy, then the binary can drift outside the host galaxy before merger. In fact, Fryer & Kalogera (1997) found evidence for kicks around 200 km s^{-1} in observed neutron star binaries with separation distances small enough to allow mergers within a Hubble time. Considering where mergers may be observed in relation to their host galaxies, Kelley et al. (2010) found that if even larger kicks are assumed, ∼360 km s^{-1}, then nearby mergers will be observed up to 1 Mpc away from their host. However, other investigators find these large kicks to be unlikely, and tend to favor models where typical mergers occur within 1–100 kpc of the host galaxy (Fryer & Kalogera 1997; Brandt & Podsiadlowski 1995; Bloom et al. 1999; Fryer et al. 1999; Belczynski et al. 2006). Observational evidence also supports the notion that most mergers occur within 100 kpc of the host galaxy. An attempt to match "hostless" short GRBs with nearby galaxies found that most of the observed short GRBs with known redshift very likely occurred within 100 kpc of their host galaxy (Berger 2010). In the same work, a comparison between the distribution of these observed short GRB offsets from their host galaxies was found to be consistent with predictions from models of NS–NS merger locations.

The *Swift* XRT has an FOV of 24 × 24 arcmin, and the UVOT has an FOV of 17 × 17 arcmin. If a merger occurs at a distance of 100 Mpc from earth, then an XRT (UVOT) observation centered on the host galaxy will observe the counterpart for any source within 300 kpc (200 kpc) of the host galaxy. This should include essentially all NS–NS mergers. Even as close to earth as 50 Mpc, it seems unlikely the merger site should be outside either FOV. Only cases where the kick velocity is extremely large, or where the host galaxy's gravitational well is much smaller than the Milky Way, allow for mergers beyond this distance.

4. CONCLUSIONS

The high fraction of short GRBs with X-ray band afterglows, and the potentially bright fluxes associated with them, make the *Swift* X-ray band an attractive wavelength to seek EM counterparts to NS–NS and NS–BH mergers. An imaging, wide field, soft X-ray band detector with a fast response to TOO requests is required. In the best case, the X-ray facility FOV would be at least 3 deg wide to match the scale of LIGO/Virgo position uncertainty. However, given the full range of requirements, the *Swift* satellite seems to be the strongest candidate facility that is currently in operation. This paper discussed two possible search strategies, which would likely be applicable under different sets of circumstances.

During the early years of advanced GW detectors, around 2015–2018, Advanced LIGO and Advanced Virgo are likely to operate at sensitivities less optimal than their design curves. The sky-average range for NS–NS mergers will be perhaps 50–100 Mpc. Under these circumstances, the large (∼100 deg^2)

position uncertainty associated with a LIGO/Virgo error box may be dramatically reduced through the use of a galaxy catalog. The *Swift* observatory could then search for an X-ray counterpart by imaging a few tens of galaxies over the course of a day, with exposures around a kilosecond. With this procedure, any on-axis afterglow should be detectable, and so it should be possible to make a detection, or else place limits on the beaming angle of short GRBs. Moreover, while the XRT searches for an afterglow, the UVOT will simultaneously obtain data across the band where kilonova emission is expected, imaging down to around magnitude 22, sufficiently deep to image a kilonova at 100 Mpc. Kilonovae are expected to emit isotropically, and so could be observable even for off-axis merger events, suggesting that this observable could accompany LIGO/Virgo triggers more often than afterglow emission. During this period, the "best guess" estimate for LIGO/Virgo detected mergers is only a few per year, so it seems plausible to follow-up every high significance trigger in this manner.

As the GW detectors mature and reach their design sensitivity, the galaxy catalog is likely to become a less useful tool. This means that instead of representing the error box with $\sim$30 pointings, it will be necessary to use hundreds of XRT tilings to cover the error box. To complete such an ambitious observing plan in a limited period of time requires sacrificing sensitivity, and the 100 s observations would be only barely deep enough to detect on-axis afterglows, and would likely be unable to detect kilonovae. On-axis afterglows are only expected to accompany $\leqslant$10% of LIGO/Virgo detections, and the detection rate in this period could be $\geqslant$40 per year. Under these circumstances, it seems unreasonable to expect an orbiting facility to follow-up every GW trigger. On the other hand, all-sky GRB monitors, most notably the *Fermi* GBM, continuously observe a large fraction of the sky, and so effectively select which LIGO/Virgo triggers are most likely to have soft-band X-ray afterglows. Coincidences between a mature Advanced LIGO/Virgo network and GBM should occur at the one per year level, an estimate that comes from the observed GRB population, and so is independent of large uncertainties in population synthesis or the GRB jet opening angle (Coward et al. 2012; Chen & Holz 2012). A coincidence between GBM and the LIGO/Virgo network will be an exciting event, and so obtaining the precise position, host galaxy, and red shift information only obtainable through an afterglow observation will be well worth the effort. Once the LIGO/Virgo network reaches its full design sensitivity, with an average NS–NS inspiral horizon of around 200 Mpc, a sensible plan with the *Swift* X-ray observatory would be to only respond to triggers in coincidence with a GRB observation. In this era ($\sim$2018), it is even possible that a fourth GW detector site will be operational, and so reduce the sky area that needs to be searched.

We are grateful for fruitful discussions and feedback from Lindy Blackburn, David Burrows, Thomas Dent, Brennan Hughey, Susan Kassin, Takanori Sakamoto, and Peter Shawhan. J.K. is supported by an appointment to the NASA Postdoctoral Program at Goddard Space Flight Center, administered by Oak Ridge Associated Universities through a contract with NASA. This work made use of data supplied by the UK Swift Science Data Centre at the University of Leicester and data obtained from the High Energy Astrophysics Science Archive Research Center (HEASARC), provided by NASA's Goddard Space Flight Center.

REFERENCES

Abadie, J., Abbott, B. P., Abbott, R., et al. 2010, Class. Quantum Gravity, 27, 173001
Abadie, J., Abbott, B. P., Abbott, R., et al. 2012a, A&A, 541, A155
Abadie, J., Abbott, B. P., & Abbott, R. 2012b, A&A, 539, A124
Abadie, J., Abbott, B. P., Abbott, R., et al. 2012c, ApJ, accepted (arXiv:1205.2216)
Abbott, B. P., Abbott, R., Acernese, F., et al. 2010, ApJ, 715, 1438
Accadia, T., Acernese, F., Alshourbagy, M., et al. 2012, J. Instrum., 7, 3012
Barthelmy, S. D., Barbier, L. M., Cummings, J. R., et al. 2005, Space Sci. Rev., 120, 143
Belczynski, K., Perna, R., Bulik, T., et al. 2006, ApJ, 648, 1110
Bell, E. F., & de Jong, R. S. 2001, ApJ, 550, 212
Bell, E. F., McIntosh, D. H., Katz, N., & Weinberg, M. D. 2003, ApJS, 149, 289
Berger, E. 2010, ApJ, 722, 1946
Berger, E. 2011, New Astron. Rev., 55, 1
Bloom, J. S., Sigurdsson, S., & Pols, O. R. 1999, MNRAS, 305, 763
Brandt, N., & Podsiadlowski, P. 1995, MNRAS, 274, 461
Briggs, M. S., Connaughton, V., Meegan, C. A., et al. 2009, in AIP Conf. Ser. 1133, Gamma-Ray Burst: Sixth Huntsville Symposium, ed. C. Meegan, C. Kouveliotou, & N. Gehrels (Melville, NY: AIP), 40
Burrows, D. N., Hill, J. E., Nousek, J. A., et al. 2005, Space Sci. Rev., 120, 165
Chen, H.-Y., & Holz, D. E. 2012, arXiv:1206.0703
Coward, D., Howell, E., Piran, T., et al. 2012, arXiv:1202.2179
Coward, D. M., Gendre, B., Sutton, P. J., et al. 2011, MNRAS, 415, L26
Dalal, N., Holz, D. E., Hughes, S., & Jain, B. 2006, Phys. Rev. D, 74, 063006
Evans, P. A., Beardmore, A. P., Page, K. L., et al. 2007, A&A, 469, 379
Evans, P. A., Beardmore, A. P., Page, K. L., et al. 2009, MNRAS, 397, 1177
Evans, P. A., Fridriksson, J. K., Gehrels, N., et al. 2012, arXiv:1205.1124
Fairhurst, S. 2011, Class. Quantum Gravity, 28, 105021
Fong, W.-f., Berger, E., Margutti, R., et al. 2012, ApJ, 756, 189
Fox, D. B., Frail, D. A., Price, P. A., et al. 2005, Nature, 437, 845
Fryer, C., & Kalogera, V. 1997, ApJ, 489, 244
Fryer, C. L., Woosley, S. E., & Hartmann, D. H. 1999, ApJ, 526, 152
Fuhrmeister, B., & Schmitt, J. H. M. M. 2003, A&A, 403, 247
Gehrels, N., Chincarini, G., Giommi, P., et al. 2004, ApJ, 611, 1005
Gehrels, N., Sarazin, C. L., O'Brien, P. T., et al. 2005, Nature, 437, 851
Gibson, R. R., & Brandt, W. N. 2012, ApJ, 746, 54
Goriely, S., Bauswein, A., & Janka, H.-T. 2011, ApJ, 738, L32
Greiner, J., Hartmann, D. H., Voges, W., et al. 2000, A&A, 353, 998
Harry, G. M., & LIGO Scientific Collaboration., 2010, Class. Quantum Gravity, 27, 084006
Hurley, K., Briggs, M., Connaughton, V., et al. 2011, in Proc. of 2011 Fermi Symposium, ed. A. Morselli (Rome, Italy)
Kanner, J., Huard, T. L., Marka, S., et al. 2008, Class. Quantum Gravity, 25, 184034
Kelley, L. Z., Ramirez-Ruiz, E., Zemp, M., Diemand, J., & Mandel, I. 2010, ApJ, 725, L91
Klimenko, S., Vedovato, G., Drago, M., et al. 2011, Phys. Rev. D, 83, 102001
Kulkarni, S. R. 2005, arXiv:astro-ph/0510256
Kuroda, K. LCGT Collaboration. 2010, Class. Quantum Gravity, 27, 084004
Li, L.-X., & Paczyński, B. 1998, ApJ, 507, L59
Mateos, S., Warwick, R. S., Carrera, F. J., et al. 2008, A&A, 492, 51
Meegan, C., Lichti, G., Bhat, P. N., et al. 2009, ApJ, 702, 791
Metzger, B. D., & Berger, E. 2012, ApJ, 746, 48
Metzger, B. D., Martínez-Pinedo, G., Darbha, S., et al. 2010, MNRAS, 406, 2650
Moretti, A., Perri, M., Capalbi, M., et al. 2007, Proc. SPIE, 6688, 66880G
Nissanke, S., Holz, D. E., Hughes, S. A., Dalal, N., & Sievers, J. L. 2010, ApJ, 725, 496
Nissanke, S., Sievers, J., Dalal, N., & Holz, D. 2011, ApJ, 739, 99
Nuttall, L. K., & Sutton, P. J. 2010, Phys. Rev. D, 82, 102002
O'Shaughnessy, R., Kalogera, V., & Belczynski, K. 2010, ApJ, 716, 615
Paciesas, W. S., Meegan, C. A., von Kienlin, A., et al. 2012, ApJS, 199, 18
Piran, T., Nakar, E., & Rosswog, S. 2012, arXiv:1204.6242
Puccetti, S., Capalbi, M., Giommi, P., et al. 2011, A&A, 528, A122
Racusin, J. L., Oates, S. R., Schady, P., et al. 2011, ApJ, 738, 138
Roberts, L. F., Kasen, D., Lee, W. H., & Ramirez-Ruiz, E. 2011, ApJ, 736, L21
Roming, P. W. A., Kennedy, T. E., Mason, K. O., et al. 2005, Space Sci. Rev., 120, 95
Schutz, B. F. 2011, Class. Quantum Gravity, 28, 125023
van Eerten, H. J., & MacFadyen, A. I. 2011, ApJ, 733, L37
White, D. J., Daw, E. J., & Dhillon, V. S. 2011, Class. Quantum Gravity, 28, 085016